

Earthquakes Induced by Hydraulic Fracturing in Poland Township, Ohio

by Robert J. Skoumal, Michael R. Brudzinski, and Brian S. Currie

Abstract Felt seismicity induced by hydraulic fracturing is very rare, with only a handful of reported cases worldwide. Using an optimized multistation cross-correlation template-matching routine, 77 earthquakes were identified in Poland Township, Mahoning County, Ohio, that were closely related spatially and temporally to active hydraulic fracturing operations. We identified earthquakes as small as local magnitudes (M_L) ~ 1 up to 3, potentially one of the largest earthquakes induced by hydraulic fracturing in the United States. These events all occurred from 4 to 12 March 2014, and the rate decayed once the Ohio Department of Natural Resources issued a shutdown of hydraulic fracturing at a nearby well on 10 March. Using a locally derived velocity model and double-difference relocation, the earthquakes occurred during six stimulation stages along two horizontal well legs that were located ~ 0.8 km away. Nearly 100 stimulation stages in nearby wells at greater distances from the earthquake source region did not coincide with detected seismicity. During the sequence, hypocenters migrated ~ 600 m along an azimuth of 083° , defining a vertically oriented plane of seismicity close to the top of the Precambrian basement. The focal mechanism determined for the M_L 3 event had a vertically oriented left-lateral fault plane consistent with the earthquake distribution and the regional stress field. The focal mechanism, orientation, and depth of hypocenters were similar to those of the 2011 Youngstown earthquake sequence that occurred 18 km to the northwest and was correlated with wastewater injection instead of hydraulic fracturing. Considering the relatively large magnitude of the Poland Township events and the b -value of 0.89, it appears the hydraulic fracturing induced slip along a pre-existing fault/fracture zone optimally oriented in the regional stress field.

Introduction

As oil and gas well completions utilizing multistage hydraulic fracturing have become more commonplace, the potential for seismicity induced by the deep disposal of frac-related wastewater and the hydraulic fracturing process itself has become an increasingly important issue (e.g., [National Academy of Sciences \[NAS\], 2012](#)). Although it is rare for a wastewater disposal well to induce felt seismicity, the recent increase in the number of wells and volumes injected are suspected to have contributed to a substantial increase of events (local magnitude [M_L] ≥ 3) in the continental United States over the past decade (e.g., [Ellsworth, 2013](#)). Felt earthquakes caused directly by hydraulic fracturing during well stimulations are even more rare, but due to the recent enhanced scrutiny regarding the practice and more sensitive seismic monitoring tools, induced seismicity attributed to hydraulic fracturing has become more prevalent in the past few years. Although microseismicity ($M_L < 1$) is an inherent component of the hydraulic fracturing process ([Warpinski et al., 2012](#)), hydraulic fracturing has previously been well correlated to only a handful of earthquakes sequences, including the 1979 moment magnitude (M_w) 1.9 Oklahoma

([Nicholson and Wesson, 1990](#)), 2011 M_L 2.9 Oklahoma ([Holland, 2013](#)), 2011 M_L 3.8 British Columbia ([British Columbia Oil and Gas Commission \[BCOGC\], 2012](#)), 2011 M_L 2.3 England ([British Geological Survey \[BGS\], 2011](#)), and 2013 M_w 2.2 Harrison County, Ohio ([Friberg et al., 2014](#)) events. Between 5 and 14 March 2014, a series of five earthquakes ranging from M_L 2.1 to 3.0 were recorded in Poland Township, Mahoning County, Ohio, near the town of Lowellville. The epicentral locations for these events were less than 20 km southeast of the locations of the 2011–2014 Youngstown earthquake sequence (YES), a series of $M_L \sim 1.0$ –4.0 events that have been linked to a deep wastewater injection well ([Holtkamp et al., 2013](#); [Kim, 2013](#); [Skoumal et al., 2014](#)). Despite this proximity, there were no injection wells operating within 10 km of the Poland Township earthquakes. However, the earthquakes occurred within 1 km of a group of recently drilled oil and gas wells in the area, one of which (Hilcorp Energy CLL2 1H; API 3409923199) was undergoing active hydraulic fracture stimulation at the time of the M_L 3.0 seismic event. Because of this proximity, the Ohio Department of Natural Resources

(ODNR) halted completion operations at the Hilcorp well on the afternoon of 10 March 2014.

Although the ODNR subsequently announced that there was a probable connection between hydraulic fracturing and the Poland Township events, to date, there has been no detailed scientific data released that demonstrates this relationship. This study seeks to investigate the Poland Township seismicity and its potential relationship to hydraulic fracturing by employing the seismographic template-matching procedure utilized to characterize the nearby 2011–2014 YES events (Holtkamp *et al.*, 2013; Skoumal *et al.*, 2014). If it can be demonstrated that the Poland Township earthquakes were induced by hydraulic fracturing, the M_L 3.0 event in the sequence would be one of the largest earthquakes directly linked to the process (Davies *et al.*, 2013).

Data and Analysis

Our analysis followed the approach of Skoumal *et al.* (2014) that was optimized for the nearby 2011–2014 YES. Data were obtained using Incorporated Research Institutions for Seismology Data Management Center Web Services, interpolated to 40 samples/s then band-pass filtered between 5 and 15 Hz. Templates of 37 s length were created from earthquakes identified by the ODNR, Lamont Doherty Earth Observatory (LDEO), and the U.S. Geological Survey (USGS) National Earthquake Information Center (NEIC). Templates began 10 s before the P -wave arrival on vertical components and 10 s before S -wave arrival on horizontal components. Cross-correlation coefficients (CCC) were calculated by correlating the template with years of data by shifting one datum at a time for each station and component. When executed in parallel with a peak usage of 72 simultaneous workers, we can achieve over 10^8 correlations/s, which allowed us to run templates through all available data in under an hour. We sum the CCC values across the network, taking into account the lag values between different station components established in the template event arrival times. For example, if O56A-BHE has an S -wave arrival 5 s later than N54A-BHE, the CCC values from O56A-BHE starting at 5 s are added to the CCC values from N54A-BHE starting at 0 s. Normalized network CCC (NNCCC) values were produced by dividing the sum of normalized CCC values for all stations and components by the number of contributing channels. We set an initial threshold of 15 times the median absolute deviation (MAD) of the daily NNCCC. Correlating a randomly generated template against a random year-long signal at 40 samples/s would result in approximately one false positive based on the theoretical statistics of $15 \times \text{MAD}$. We then sought to lower the $15 \times \text{MAD}$ threshold to increase the number of matched events without changing the temporal trend of matched events, while also maintaining coherent seismic arrivals.

Considering the presence of the EarthScope Transportable Array, various station combinations were investigated to determine the template that produced the highest number of positive detections and minimized false positives. Although

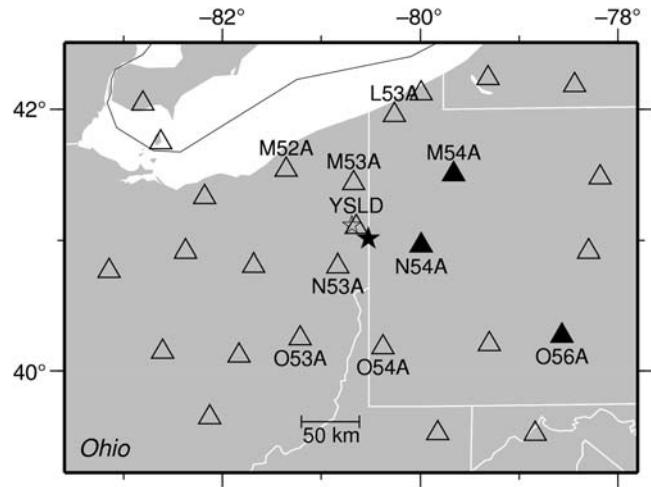


Figure 1. Regional map identifying seismic stations (triangles). Black stations were used for template matching, labeled stations were used to determine an absolute location of Poland Township sequence (star), and all stations shown were used in the relocation of matched events. The Youngstown sequence (Skoumal *et al.*, 2014) occurred at the northwestern edge of the station YSLD triangle.

stations N53A and YSLD were the closest to the source region (Fig. 1), large and repetitive noise at these stations had detrimental effects on template-matching performance. The ideal network consisted of stations M54A, N54A, and O56A, which was the same combination found by Skoumal *et al.* (2014). The stations in the most successful template were installed in early November 2010, such that scans with this template were run from 6 November 2010 to 6 May 2014.

The earthquakes returned from the template-matching process were located through a combination of absolute and relative location techniques. The absolute location of the largest event (M_L 3.0, 10 March 2014, 06:26:42) was determined using *elocate* (Herrmann, 2004). The inversion used the manually picked arrival times of the clearest P and S waveforms on 10 stations (labeled stations, Fig. 1). We considered using the 1D velocity models for the nearby Youngstown region presented by Kim (2013), as the two models developed for that study were based on sonic logs in the area and were appropriate for the local recordings used in that study (Table 1). However, our study used regional stations such that seismic waves recorded in our study primarily sample deeper depths. Faced with a similar issue, similar studies have sought to identify a model that would be more appropriate for this case (Holtkamp *et al.*, 2013; Skoumal *et al.*, 2014). Beginning from the northeastern Ohio velocity model, the parameters were adjusted through forward modeling to reduce the variance and the bootstrap error estimates (Table 1). An additional lower crustal layer was added to help fit arrival times at more distal stations. Considering that the bedrock units in this portion of Ohio dip gently ($\sim 1^\circ$) to the southeast into the Appalachian basin (Baranoski, 2013), the velocity models were adjusted to accommodate

Table 1
Layered Velocity Models Considered in Determining
Locations of the Poland Township Earthquake Sequence

| Model | Depth (km) | V_P (km/s) | V_S (km/s) |
|-------------------------|------------|--------------|--------------|
| Preferred | 0.0 | 4.50 | 2.60 |
| | 3.10 | 5.94 | 3.43 |
| | 4.00 | 6.12 | 3.54 |
| | 10.0 | 6.60 | 3.82 |
| | 40.0 | 8.10 | 4.68 |
| Adjusted Kim (2013) A | 0.0 | 3.86 | 2.19 |
| | 1.19 | 4.98 | 2.83 |
| | 2.46 | 6.13 | 3.48 |
| | 3.10 | 6.15 | 3.49 |
| | 10.0 | 6.62 | 3.76 |
| Adjusted Kim (2013) B | 41.0 | 8.10 | 4.60 |
| | 0.0 | 3.86 | 2.23 |
| | 1.19 | 4.98 | 2.88 |
| | 2.46 | 6.13 | 3.54 |
| | 10.0 | 6.62 | 3.83 |
| Adjusted northeast Ohio | 41.0 | 8.10 | 4.68 |
| | 0.0 | 4.50 | 2.60 |
| | 3.10 | 6.12 | 3.54 |
| | 10.0 | 6.62 | 3.83 |
| | 41.0 | 8.10 | 4.68 |

the thicker formations and deeper tops reported in a vertical well within 1 km from the Poland Township epicenters (CLL1 1V; API 3409923185) and the deeper basement contact estimated for the well location (Table 1). The absolute location errors were determined using bootstrapping, removing one station at a time from the location process and using the standard deviation as the error estimate (Efron, 1979) (Table 2).

The relative locations of all matched events were determined using a larger network of 26 stations (Fig. 1) following the approach of Skoumal *et al.* (2014). Lag times and correlations were generated between the template and each matched event using a 10 s long window that began 4 s prior to the P -wave arrival on vertical components and 4 s prior to the S -wave arrival on horizontal components. This process produced P - and S -wave arrival times and weights (proportional to the correlation coefficient) for all matched events, which were used with *elocate* and the velocity model to determine an initial set of catalog locations. A full set of lag and correlation matrices between all events for all channels were then used in a hypoDD double-difference algorithm to deter-

mine the relative locations of the events (Waldhauser and Ellsworth, 2000; Waldhauser, 2001). The median relative locations errors we found based on bootstrapping estimation were ± 11 m horizontally and ± 89 m vertically (Table 2). When interpreting maps and cross sections, we focus only on events with horizontal and vertical relative location uncertainties less than ± 10 m and ± 100 m, respectively. Relocated hypocenters were pinned to the absolute location determined for the largest event, preserving the relative locations.

We determined M_L through a Richter scale approach:

$$M_L = \log_{10}[A/A_0].$$

For each station and component in our template, we calculated the median scale factor (A_0) using the filtered S -waveform amplitudes (A) and catalog magnitudes for all six events reported by the ODNR/LDEO/NEIC. For each matched event, we calculated a magnitude from the scale factor and S -waveform amplitude at each station and component and took the median value as our final magnitude.

To gain additional perspective on the stresses at work in this earthquake sequence, we calculated a fault-plane solution for the largest event, which was just large enough to make reliable identifications of first-motion polarities (nominally, $M_L \geq 3.0$). To determine the fault-plane solution, we used FOCMEC, which performed a grid search of the focal sphere based on user-specified criteria (Snoke, 2003). Input files for FOCMEC were assembled using event-station information and careful examination of first-motion polarities in all available waveforms. Takeoff angles were estimated using the pseudobending method within tomoDD (Zhang and Thurber, 2003). We used the default criteria within FOCMEC to calculate a set of fault-plane solutions for the lowest number of allowable polarity errors, and then took the median of these solutions as the fault-plane solution for a specific event.

Results

Using an initial threshold of $15 \times \text{MAD}$, our template-matching procedure identified 60 similar events that all occurred between 4 and 12 March 2014 (Fig. 2; Table 3). There were no matches before 16:23 on 4 March 2014, indicating no similar seismicity since recording began in November

Table 2
Performance of Layered Velocity Models in Determining Locations of the Poland Township Earthquake Sequence

| Model | Preferred | Adjusted Kim (2013) A | Adjusted Kim (2013) B | Adjusted Northeast Ohio |
|--------------------------------------------------------------|-----------|-----------------------|-----------------------|-------------------------|
| Root mean square residual of cross-correlation waveforms (s) | 0.0084 | 0.080 | 0.0084 | 0.0077 |
| Double-difference hypocentral location variance (s) | 44.3 | 45.6 | 45.7 | 45.2 |
| Median bootstrap horizontal error estimate (°) | 0.00010 | 0.00033 | 0.00029 | 0.00013 |
| Median bootstrap vertical error estimate (km) | 0.089 | 0.11 | 0.19 | 0.083 |

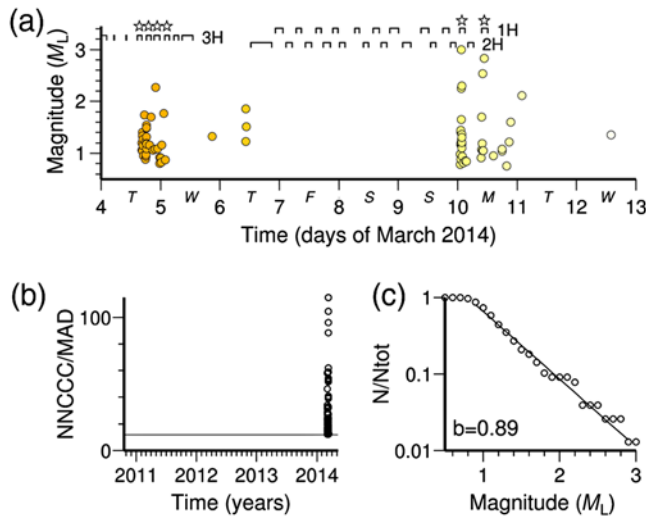


Figure 2. Summary of template-matching results. (a) Magnitudes of matched events, shaded based on time. For well operations during this period (1H, 2H, 3H), the timing of the stimulations is marked across the top. Stars indicate stages that correlate with matched seismicity. The x axis is plotted in local time for comparison with daily operations. (b) Normalized network cross-correlation coefficient (NNCCC) over time, plotted with respect to the median absolute deviation (MAD) value. The horizontal line marks $12 \times \text{MAD}$, which is our threshold for detection. (c) Magnitude–recurrence relationship with calculated b -value. The color version of this figure is available only in the electronic edition.

2010 (Fig. 2b). When the threshold was lowered to $12 \times \text{MAD}$, 77 events were all identified during 4–12 March 2014. Thresholds below $12 \times \text{MAD}$ resulted in a few spurious matches in the years prior to the sequence based on visual inspection, thus the 77 events from the $12 \times \text{MAD}$ threshold were utilized for the remainder of our study. Based on the M_L that we calculated for the 77 detected events, we estimated a magnitude of completeness at M_L 0.85 (Fig. 2c), comparable to that obtained for the nearby Youngstown sequence with similar processing (Skoumal *et al.*, 2014). We also calculated a Gutenberg–Richter b -value for the entire Poland Township sequence, which is 0.89 with the maximum-likelihood estimate (Fig. 2c). Seismicity directly resulting from hydraulic fracturing is expected to have a b -value of ~ 2 (Maxwell *et al.*, 2009; Wessels *et al.*, 2011), whereas seismicity associated with fluid injection is expected to have a b -value < 1 (Lei *et al.*,

2008; Bachmann *et al.*, 2014). For example, the overall Youngstown sequence b -value was 0.82 (Skoumal *et al.*, 2014). Seismicity directly resulting from hydraulic fracturing is expected to be $M_w < 1$ (Warpinski *et al.*, 2012). The relatively large magnitude of the events and the low b -value support the notion that the majority of earthquakes we detected were not signatures of actual hydraulic fracturing. Instead, the sequence could represent slip on a pre-existing fault during well stimulation.

We turned to the earthquake locations to investigate this hypothesis. The absolute location we obtained for the 06:26 10 March 2014 best-recorded event was approximately 1 km east of the location reported by ODNr/LDEO/NEIC (Fig. 3). Although the original location for the event placed it near horizontal wells that had been completed by Hilcorp in 2012–2013 (CCL1), the location we determined placed it near horizontal wells that were proposed by Hilcorp for operation in 2014 (CCL2) (ODNR, 2014b). After completing our initial relocation location analysis, we contacted ODNr and were informed that well CCL2-1H was being hydraulically fractured when the largest event occurred.

Once the full well stimulation reports were available approximately four months afterward, we identified the earthquakes corresponded to hydraulic fracturing stages on legs 1H and 3H (Fig. 2a). The 1H and 3H stages with coincident seismicity were the most northeastern stages that had been hydraulically fractured (Fig. 3), but the two northwesternmost stages of 3H did not correlate with earthquakes. Note that 6H stages reach as far north as the 1H stages (Fig. 3), but there are no earthquakes during these hydraulic fracturing stages on 23 February 2014. Following termination of completion operations on the afternoon of 10 March 2014, there was a marked decline in seismicity, with only six events in the following 12 hours and only a single event (13:58 12 March) over approximately the next two months.

Considering events with the lowest location uncertainties (horizontal < 10 m; vertical < 100 m), the western portion of our relocated epicenters primarily occurred during stimulation of well 3H and immediately following it (4–6 March). The eastern portion of our relocated epicenters primarily occurred during stimulation of well 1H (10 March). The events following termination of stimulations tended to occur in the western portion. In particular, the event on

Table 3
Largest Earthquakes Identified in the Poland Township Earthquake Sequence

| Date (yyyy/mm/dd) | Time (UTC) (hh:mm:ss) | Latitude (°) | Longitude (°) | Depth (km) | M_L |
|----------------------|--------------------------|------------------------|-------------------------|-----------------|-------|
| 2014/03/05 | 03:05:16 | 41.01339 ± 0.00005 | -80.52670 ± 0.00014 | 3.14 ± 0.09 | 2.3 |
| 2014/03/10 | 06:26:42 | 41.01380 ± 0.00006 | -80.52370 ± 0.00013 | 3.10 ± 0.09 | 3.0 |
| 2014/03/10 | 06:42:41 | 41.01408 ± 0.00005 | -80.52449 ± 0.00013 | 3.04 ± 0.09 | 2.3 |
| 2014/03/10 | 15:03:44 | 41.01390 ± 0.00006 | -80.52288 ± 0.00013 | 3.09 ± 0.09 | 2.5 |
| 2014/03/10 | 15:44:03 | 41.01374 ± 0.00006 | -80.52404 ± 0.00012 | 3.11 ± 0.09 | 2.8 |
| 2014/03/11 | 07:01:10 | 41.01340 ± 0.00006 | -80.52769 ± 0.00013 | 3.17 ± 0.09 | 2.1 |

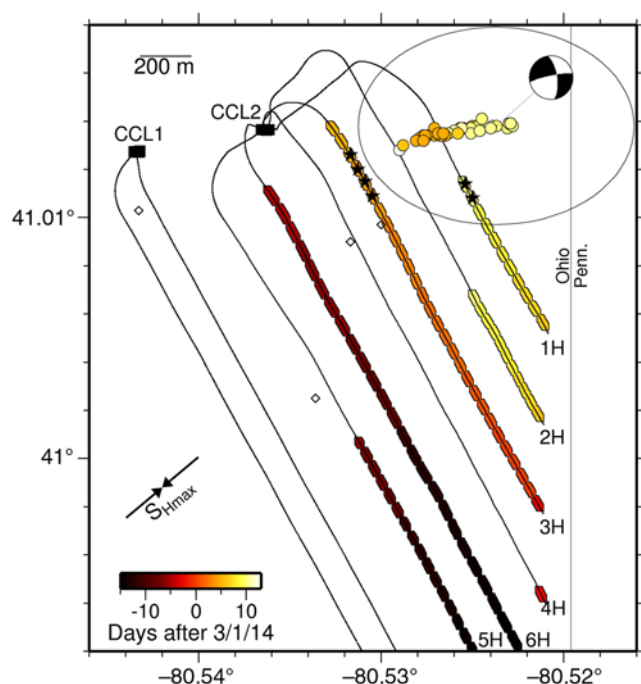


Figure 3. Map of the double-difference relocated earthquakes with the lowest relative location uncertainties shaded according to time. Curved lines indicate horizontal drilling well paths, with stimulation stages shaded using the same time scale. Stars indicate stages that correlate with times of seismicity. Well CCL1 was completed in 2013. The focal mechanism is from the 10 March 2014 06:26 M_L 3 event. Diamonds are the reported ODNR/LDEO/NEIC locations of the largest earthquakes in this sequence. The color version of this figure is available only in the electronic edition.

12 March occurred at the western end of our epicenters and appears to be an aftershock of the 4–6 March sequence.

This suggested that slip migration away from the well ceased after hydraulic fracturing operations were halted. The waveforms supported the location trends over time, as events during 3H stimulation and immediately following had distinctly similar waveforms (Fig. 4), with the largest arrival at 17.5 s, a small early arrival at 17.0 s, and a prominent third arrival at 18.5 s. Waveforms during 1H stimulation were similar overall, the early arrival at 17.0 s was significantly larger, and the late arrival at 18.5 s was smaller. Waveforms recorded after 1H stimulation was terminated returned to the pattern seen during 3H stimulation with larger second and third arrivals.

Given the calculated depths, geologic cross sections through the study region showed that the events most likely occurred near the basement contact based on comparisons between our relocated hypocenters, the well paths, and estimated basement depths (Fig. 5). The borehole deviation survey reports for wells 1H and 3H indicate the horizontal trajectories through the target interval (the Ordovician Point Pleasant formation). Using the depth error bars determined for the 10 March M_L 3.0 event as a guide, the range of calculated depths for the 77 earthquakes identified as part of this

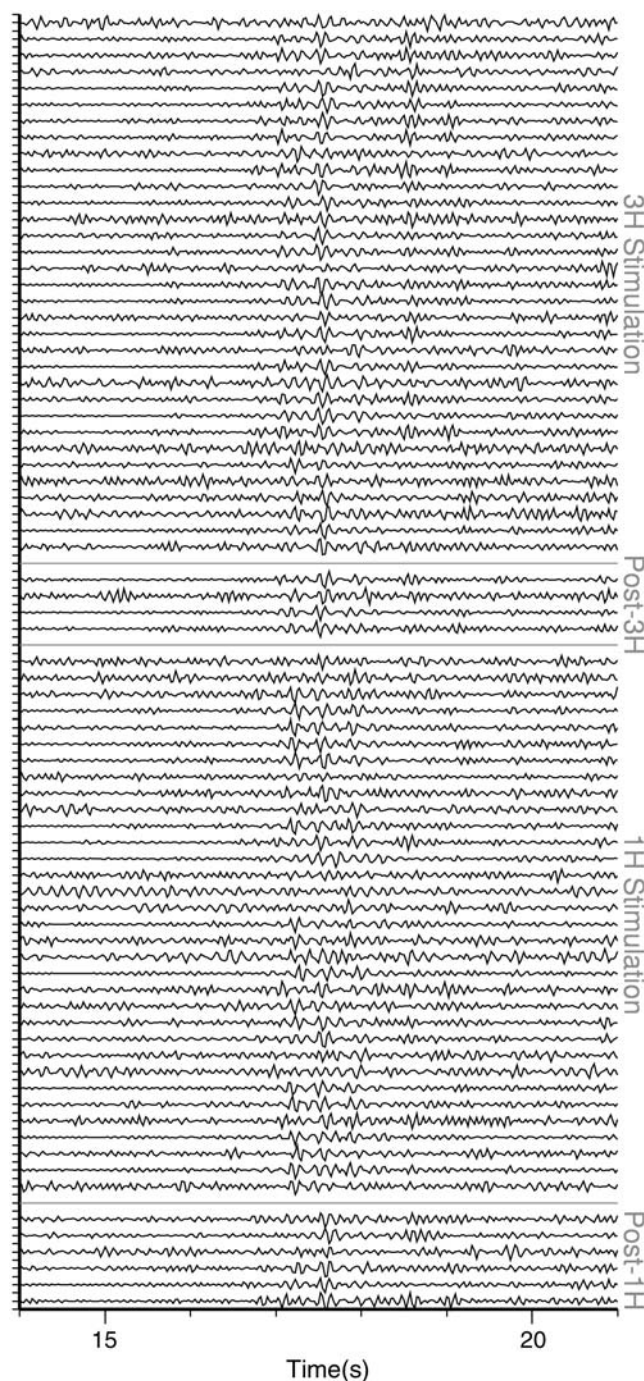


Figure 4. Horizontal component (BHN) waveforms at station N54A for the 77 identified events (in chronological order from top to bottom). Gray lines divide key phases of well stimulation. All traces are normalized to their maximum amplitude.

study indicate the events most likely occurred within 200 m of the Precambrian basement, approximately 500 m below the target interval. Note that while our absolute depth uncertainty was ± 280 m, our best-fitting absolute depth was at the basement contact, and our relative depth uncertainty was ± 150 m. This relocated hypocentral distribution indicated that many, if not all, events in the sequence occurred along

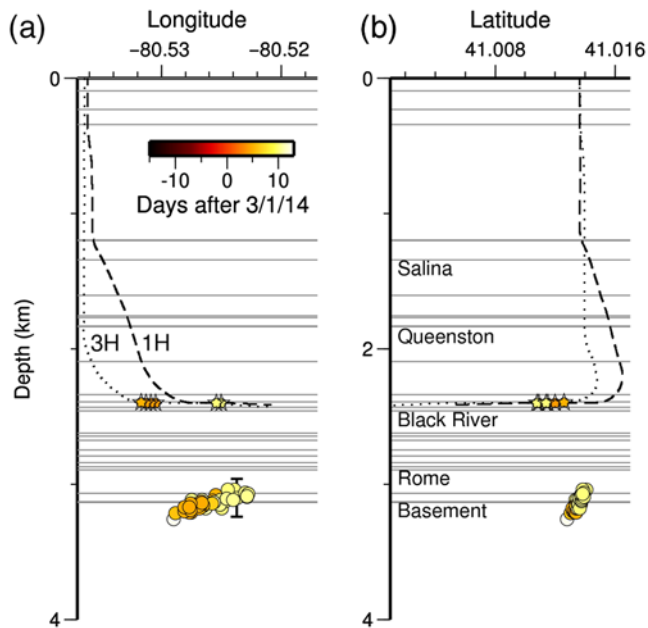


Figure 5. (a) East–west and (b) north–south cross sections of the double-difference relocated seismicity (shaded by time, as in Figure 3). Absolute depths were based on the 10 March 2014 06:26 M_L 3 event, with the vertical error bar through this event based on bootstrap estimates of depth uncertainty indicating the events most likely occurred near the Precambrian basement contact. Horizontal gray lines mark key strata. The dashed and dotted black lines were the paths of wells 1H and 3H, respectively, targeting the Point Pleasant formation. No exaggeration is included. The color version of this figure is available only in the electronic edition.

a roughly vertical, east–west-oriented fault (or faults) with likely basement involvement.

In order to confirm the possible geometry of the potential fault system, we calculated the fault-plane solution for the largest 10 March 2014 M_L 3.0 event. The fault-plane solution was based on the best 20 P -wave arrivals (Fig. 6) and revealed a near-vertical (82° dip) east–northeast–west–southwest-oriented fault plane that had nearly the same strike (258°) as that outlined by the distribution of hypocenters (262°). The similarity to the previous 31 December 2011 M_w 4.0 of the YES (strike 265° , dip 72° N; Kim, 2013) indicated the potential for a consistent basement fault fabric across Mahoning County, Ohio. The focal mechanism and waveform similarity indicated that the Poland Township earthquake sequence occurred as a series of left-lateral displacements on a near-vertical fault.

The comparison of timing and 3D locations of the best-located earthquake hypocenters and well stimulations help demonstrate the apparent relationship. To further illustrate this, we examined each well stimulation stage and plotted the average distance from the portion of the well stimulated to the hypocenters during that stage or up to 1 hr after (Fig. 7). If earthquakes did not occur during that stage, we plot the average distance from the stage to the five earthquakes closest in time. Although this is still a simplistic comparison, it

illustrates the six stimulations that correlated in time with seismicity were at distances of 750–850 m. None of the nearly 100 other stimulation stages in the CCL2 wells at distances larger than 850 m from the earthquake source region coincided with detected seismicity. The lack of seismicity coincident with the northernmost stages at 6H indicates the seismogenic fault is limited in extent and does not reach that far west. Further support for this can be found in the limited number of correlations at well 3H, with the two northernmost stages apparently too far from the fault to generate seismicity.

Discussion

The temporal and spatial proximity of the Poland Township earthquakes to active hydraulic fracturing operations strongly suggested that the stimulation process triggered the seismic events. In addition, the relatively large magnitudes compared with hydraulic fracturing microseismicity and calculated b -value of the earthquakes indicated slip on a pre-existing fault as opposed to the creation of a new fault. Pore-fluid pressures may have been elevated due to hydraulic fracture fluids or pressurized formation waters that entered a pre-existing fault or fracture zone, either as a result of intersection with the well borehole (Hulsey *et al.*, 2010) or along natural fractures induced during well stimulation (Wolhart *et al.*, 2005; Davies *et al.*, 2013). In this interpretation, the increase of fluid pressure reduced effective normal stress on the fault surface and permitted fault slip (Healy *et al.*, 1968; Simpson, 1986; Nicholson and Wesson, 1990; Zoback and Harjes, 1997). The approximately east–northeast–west–southwest orientation of the proposed fault was within the range of optimal orientations for reactivation, given the northeast–southwest orientation of regional SH_{\max} in eastern Ohio (Zoback, 1992).

We note that the well 3H stimulation report shows evidence for a “screen-out” in the stage immediately before the earthquakes began, which may have occurred as fluids injected to produce hydraulic fractures entered a permeable fault or fracture zone. The escaping fluids could have caused induced fractures closer to the well bore to close, resulting in the elevated well-bore pressures. Although this scenario is highly speculative, the report from ODNr shows likely screen-out-related shut downs in stimulation activities between 02:00 and 10:20 (local time) on 4 March, approximately 6 hrs prior to our first detected earthquake (16:23, 4 March).

Alternatively, fluid pressure may have also increased through poroelastic stress coupling between fractured lithologies and formation fluids (Davies *et al.*, 2013; Lacazette and Geiser, 2013). As such, seismic events associated with hydraulic fracture-related fault reactivation can occur close to the borehole or up to several 100 s of meters from a well (Davies *et al.*, 2013). Tomographic imaging of areas adjacent to wells undergoing hydraulic fracturing suggest that pre-existing structures can be seismically activated as much as 1 km both horizontally and vertically from the borehole

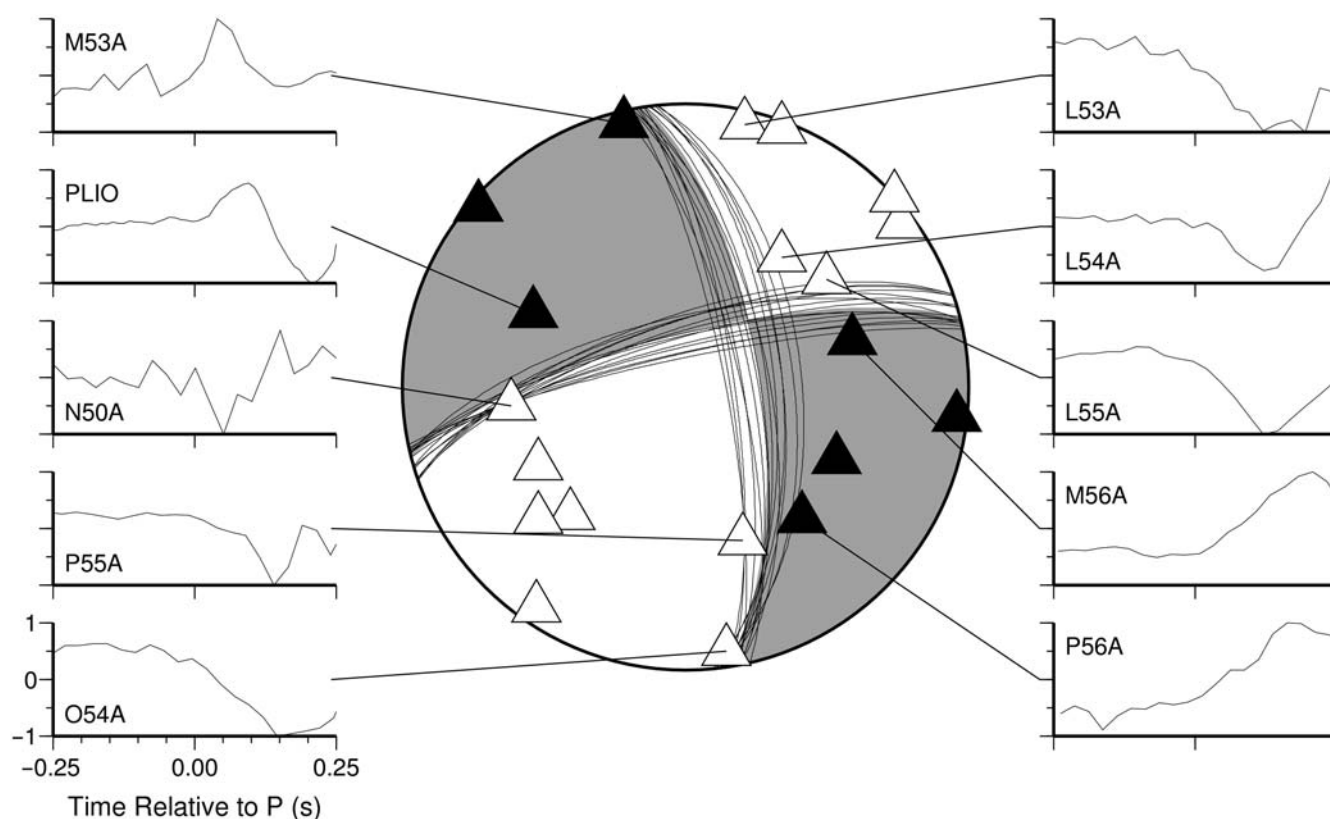


Figure 6. Fault-plane solution and selected first-arrival waveforms for the 06:26 10 March 2014 M_L 3 earthquake. Triangles on the focal sphere show station polarity data for compressional (black) and dilatational (white) first motions. Seismograms show 0.25 before and after the picked P -wave arrival time at each station.

(Lacazette and Geiser, 2013). This observation could explain the spatial distribution of the Poland Township earthquakes that indicated hydraulic fracturing was likely influencing faults up to 850 m away from the well stimulations (Fig. 7).

Our findings were similar to those from a study of 38 earthquakes (M_L 2.2–3.8) between April 2009 and December 2011 identified by Natural Resources Canada in the Horn River basin in northeast British Columbia (BCOGC, 2012). Dense arrays of 20 and 151 stations were installed in the Etsho and Tattoo areas of the basin, respectively, and a combined set of 254 events of $M_L \geq 2.0$ was identified. Fault mapping in the area found abundant pre-existing faults. BCOGC concluded these events were the result of fluids injected from nearby hydraulic fracturing operations that activated the pre-existing faults. In both the Etsho–Tattoo and Poland Township areas, there was no reported seismicity prior to the hydraulic fracturing operations. Although the Etsho–Tattoo operations had legs that were drilled ~ 1 km from each other, a leg that resulted in extensive seismicity could be adjacent to others that had little to no attributed seismicity. Almost all seismicity from the Etsho–Tattoo sequences were confined below the target interval and occurred horizontally adjacent to hydraulic fracturing operations. Further analysis of the largest events aligned along a cluster of seismicity oriented within 30° of the principal horizontal stress direction below the res-

ervoir (Baig *et al.*, 2013). This alignment suggested that the stress redistribution from hydraulic injection is sufficient to cause larger-scale, optimally oriented faults to slip in surrounding formations.

In April 2014, following the Poland Township earthquake sequence, the ODNR issued new regulations that will apply to new horizontal wells in Ohio located within three miles of a known fault or previously identified seismicity $M_w \geq 2.0$ (ODNR, 2014a). Although we did not have access to any proprietary data from the operator, to the best of our knowledge, these new regulations would not have applied to the Hilcorp Energy wells in Poland Township, as no known fault or historical seismicity had been identified in the area prior to hydraulic fracturing. This fact highlights the potential of rapid regional template-matching techniques that can analyze any seismicity that may be related to ongoing hydraulic fracturing operations to determine if they are part of a larger repeating sequence. Our characterization of the Poland Township sequence demonstrated the viability of the template-matching approach, as we were able to complete the template-matching process within 1 hr of being informed of the 10 March 2014 M_L 3.0 event. Had we been informed of the M_L 2.1 earthquake that occurred on 5 March, we would likely have identified the majority of the $M_L < 2.0$ earthquakes that occurred during the first couple days of the

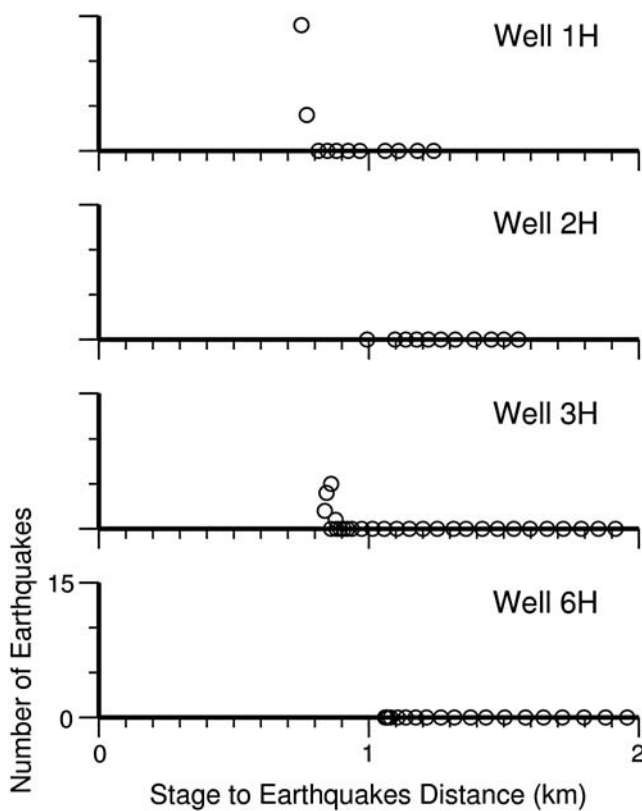


Figure 7. Estimate of 3D distance from stimulation stage in horizontal wells to relocated earthquake hypocenters. Only the earthquakes with the lowest relative location uncertainties are considered (Fig. 3).

sequence. If hydraulic fracturing of the CLL2 wells had been terminated at that point, the more broadly felt events that occurred later in the earthquake sequence might have been prevented. The seismic network utilized for our template matching will continue to be applicable for eastern Ohio and surrounding regions, as the three EarthScope Transportable Array stations used in this study were adopted as permanent components of the Pennsylvania seismic network.

Conclusions

Using an optimized multistation cross-correlation template-matching routine, 77 events were identified in two temporal clusters during 4–12 March 2014 that temporally and spatially coincided with nearby hydraulic fracturing operations. We identified earthquakes as small as $M_L \sim 1$ up to 3, some of the largest earthquakes induced by hydraulic fracturing in the United States. Using a locally derived velocity model, a combination of absolute and double-difference relocations indicate the events less than ~ 850 m from two lateral wells that were actively hydraulic fracturing. The relocated events outline a fault with a strike of 262° near the top of the crystalline Precambrian basement. A focal mechanism calculated for the M_L 3 event has a left-lateral fault plane with nearly the same azimuth as the earthquake distribution

that appears to be optimally oriented within the regional stress field. The relatively large magnitude of these events and the b -value of 0.89 suggested slip occurred along a pre-existing fault that was induced to rupture by nearby hydraulic fracturing.

Optimized template matching utilizes high-quality reliable stations within pre-existing seismic networks and is therefore a cost-efficient monitoring strategy for identifying and characterizing potentially induced seismic sequences. This is particularly important in places like Ohio, where new state regulations on activities related to hydraulic fracturing are being implemented based on seismicity patterns.

Data and Resources

Seismic data and earthquake catalogs were obtained from the Incorporated Research Institutions for Seismology Data Management Center at www.iris.edu (last accessed March 2014). Plots were made using the Generic Mapping Tools version 4.2.1 (www.soest.hawaii.edu/gmt/, last accessed June 2014; Wessel and Smith, 1998).

Acknowledgments

Support for this work was provided by National Science Foundation Grant EAR-0847688 (MB). We benefitted from discussions with Steve Holtkamp, Paul Friberg, Chris Grope, Tom Serenko, Mike Hansen, Mike Angle, and many others at the Ohio Department of Natural Resources. Paul Friberg, Art McGarr, and Ivan Wong provided constructive reviews of the manuscript that significantly improved this publication.

References

- Bachmann, C. E., W. Foxall, and T. Daley (2014). Comparing induced seismicity on different scales, *Proceedings, Thirty-Ninth Workshop on Geothermal Reservoir Engineering*, Stanford University, Stanford, California, 24–26 February 2014.
- Baig, A., T. Urbancic, and F. Viegas (2013). Characterizing felt seismicity during hydraulic fracture stimulations, *Geol. Soc. Am. Abstr. Progr.* **45**, no. 7, 841.
- Baranoski, M. T. (2013). Structure contour map on the Precambrian unconformity surface in Ohio and related basement features (version 2.0), *Columbus, Ohio Department of Natural Resources, Division of Geological Survey Map PG-23*, scale 1:500,000, 17.
- British Columbia Oil and Gas Commission (BCOGC) (2012). Investigation of observed seismicity in the Horn River basin, *Technical Rept.*, <http://www.bco.gc.ca/investigation-observed-seismicity-horn-river-basin> (last accessed June 2014).
- British Geological Survey (BGS) (2011). Blackpool earthquake, magnitude 2.3, 1 April 2011, available at <http://earthquakes.bgs.ac.uk/research/events/BlackpoolApril2011.html> (last accessed December 2014).
- Davies, R., G. Foulger, A. Bindley, and P. Styles (2013). Induced seismicity and hydraulic fracturing for the recovery of hydrocarbons, *Mar. Petrol. Geol.* **45**, 171–185.
- Efron, B. (1979). Bootstrap methods: Another look at the jackknife, *Ann. Stat.* **7**, 1–26.
- Ellsworth, W. L. (2013). Injection-induced earthquakes, *Science* **341**, doi: 10.1126/science.1225942.
- Friberg, P. A., G. M. Besana-Ostman, and I. Dricker (2014). Characterization of an earthquake sequence triggered by hydraulic fracturing in Harrison County, Ohio, *Seismol. Res. Lett.* **85**, doi: 10.1785/0220140127.
- Healy, J. H., W. W. Rubey, D. T. Griggs, and C. B. Raleigh (1968). The Denver earthquakes, *Science* **161**, no. 3848, 1301–1310.

- Herrmann, R.-B. (2004). *Computer Programs in Seismology*, Version 3.30-GSAC, http://www.eas.slu.edu/eqc/eqc_cps/CPS/CPS330.html (last accessed March 2008).
- Holland, A. (2013). Earthquakes triggered by hydraulic fracturing in south-central Oklahoma, *Bull. Seismol. Soc. Am.* **103**, no. 3, 1784–1792.
- Holtkamp, S., B. Currie, and M. Brudzinski (2013). A more complete catalog of the 2011 Youngstown, Ohio earthquake sequence from template matching reveals a strong correlation to pumping at a wastewater injection well, *AAPG Search and Discovery Article #90163, 2013 Annual Convention and Exhibition*, Pittsburgh, Pennsylvania, 19–22 May.
- Hulsey, B. J., B. Cornette, and D. Pratt (2010). Surface microseismic mapping reveals details of the Marcellus shale, *Society of Petroleum Engineers, Eastern Regional Meeting*, Morgantown, West Virginia, 13–15 October, 2010, SPE-138806-MS, 7 pp.
- Kim, W.-Y. (2013). Induced seismicity associated with fluid injection into a deep well in Youngstown, Ohio, *J. Geophys. Res.* **118**, 3506–3518, doi: [10.1002/jgrb.50247](https://doi.org/10.1002/jgrb.50247).
- Lacazette, A., and P. Geiser (2013). Comment on Davies et al., 2012—Hydraulic fractures: How far can they go? *Mar. Petrol. Geol.* **43**, doi: [10.1016/j.marpetgeo.2012.12.008](https://doi.org/10.1016/j.marpetgeo.2012.12.008).
- Lei, X., G. Yu, S. Ma, X. Wen, and Q. Wang (2008). Earthquakes induced by water injection at ~3 km depth within the Rongchang gas field, Chongqing, China, *J. Geophys. Res.* **113**, no. B10, doi: [10.1029/2008JB005604](https://doi.org/10.1029/2008JB005604).
- Maxwell, S. C., M. Jones, R. Parker, S. Miong, S. Leaney, D. Dorval, D. D'Amico, J. Logel, E. Anderson, and K. Hammermaster (2009). Fault activation during hydraulic fracturing, *SEG Technical Program Expanded Abstracts 2009*, 1552–1556, doi: [10.1190/1.3255145](https://doi.org/10.1190/1.3255145).
- National Academy of Sciences (NAS) (2012). *Induced Seismicity Potential in Energy Technologies*, Natl. Acad. Press, Washington, D.C., 225.
- Nicholson, C., and R. L. Wesson (1990). Earthquake Hazard Associated with Deep Well Injection: A report to the U.S. Environmental Protection Agency, *U.S. Geol. Surv. Bull.* **1951**, <http://pubs.usgs.gov/bul/1951/report.pdf> (last accessed June 2014).
- Ohio Department of Natural Resources (ODNR) (2014a). *Ohio Announces Tougher Permit Conditions for Drilling Activities Near Faults and Areas of Seismic Activity*, <http://ohiodnr.gov/news/post/ohio-announces-tougher-permit-conditions-for-drilling-activities-near-faults-and-areas-of-seismic-activity> (last accessed December 2014).
- Ohio Department of Natural Resources (ODNR) (2014b). *Ohio Oil & Gas Well Locator*, <http://oilandgas.ohiodnr.gov/well-information/oil-gas-well-locator> (last accessed June 2014).
- Simpson, D. W. (1986). Triggered earthquakes, *Ann. Rev. Earth Planet. Sci.* **14**, 21–42.
- Skoumal, R. J., M. R. Brudzinski, B. S. Currie, and J. Levy (2014). Optimizing multi-station earthquake template matching through re-examination of the Youngstown, Ohio sequence, *Earth Planet. Sci. Lett.* **405**, 274–280.
- Snoke, J. A. (2003). FOCMEC: FOCal MEchanism Determinations, <http://www.geol.vt.edu/outreach/vtso/focmec/> (last accessed June 2014).
- Waldhauser, F. (2001). Hypodd: A computer program to compute double-difference earthquake locations, *U.S. Geol. Surv. Open-File Rept.* **01-113**.
- Waldhauser, F., and W. L. Ellsworth (2000). A double-difference earthquake location algorithm: Method and application to the northern Hayward fault, California, *Bull. Seismol. Soc. Am.* **90**, 1353–1368.
- Warpinski, N. R., J. Du, and U. Zimmer (2012). Measurements of hydraulic-fracture-induced seismicity in gas shales, *SPE Hydraulic Fracture Technology Conference*, The Woodlands, Texas, 6–8 February 2012, Soc. Pet. Eng. Abstract 151597.
- Wessel, P., and W. H. Smith (1998). New, improved version of Generic Mapping Tools released, *Eos Trans. AGU* **79**, no. 47, 579.
- Wessels, S., M. Kratz, and A. De La Pena (2011). Identifying fault activation during hydraulic stimulation in the Barnett shale: Source mechanisms, *b* values, and energy release analyses of microseismicity, *SEG Technical Program Expanded Abstracts 2011*, San Antonio, Texas, 18–23 September.
- Wolhart, S., E. Davis, W. Roadarmel, and C. Wright (2005). Reservoir deformation monitoring to enhance reservoir characterization and management, *SEG Technical Program Expanded Abstracts 2005*, Houston, Texas, 6–11 November 2005, 2512–2515.
- Zhang, H., and C. H. Thurber (2003). Double-difference tomography: The method and its application to the Hayward fault, California, *Bull. Seismol. Soc. Am.* **93**, no. 5, 1875–1889.
- Zoback, M. D., and H.-P. Harjes (1997). Injection-induced earthquakes and crustal stress at 9 km depth at the KTB deep drilling site, Germany, *J. Geophys. Res.* **102**, no. B8, 18,477–18,491, doi: [10.1029/96JB02814](https://doi.org/10.1029/96JB02814).
- Zoback, M. L. (1992). Stress field constraints on intraplate seismicity in eastern North America, *J. Geophys. Res.* **97**, no. B8, 11,761–11,782.

Miami University
Department of Geology and Environmental Earth Science
114 Shideler Hall
Oxford, Ohio 45056
skoumarj@miamioh.edu
brudzimr@miamioh.edu
curriebs@miamioh.edu

Manuscript received 11 June 2014;
Published Online 6 January 2015